Research Article

Journal of Labelled Compounds and Radiopharmaceuticals

Received 28 January 2010, Revised 18 March 2010, Accepted 12 April 2010 Published online 18 June 2010 in Wiley Online Library

(wileyonlinelibrary.com) DOI: 10.1002/jlcr.1786

Optimizing $[^{13}N]N_2$ radiochemistry for nitrogen-fixation in root nodules of legumes

Mirjam C. K. Kasel,[a] Michael J. Schueller,[b] and Richard A. Ferrieri[b]*

Here we explored the conditions for synthesizing $[^{13}N]N_2$ in a state that is suitable for the administration to plant root nodules enabling studies of nitrogen fixation. $[^{13}N]N_2$ was prepared batchwise, starting with $[^{13}N]NO_3^-$ from the $^{16}O(p,\alpha)^{13}N$ nuclear reaction on a liquid water target. $[^{13}N]NO_3^-$ was first reduced to $[^{13}N]NH_3$ using Devarda's alloy, and then the $[^{13}N]NH_3$ was oxidized to $[^{13}N]N_2$ by hypobromite using carrier-added NH_4Cl. The amounts of carrier NH_4Cl and hypobromite were varied to determine the effects these parameters had on the radiochemical yield, and on the radiotracer specific activity. As expected, increasing the amount of carrier NH_4Cl improved the radiochemical yield. Unexpectedly, increasing the amount of excess hypobromite from 1.6-fold to 6-fold molar equivalents (relative to NH_4Cl) improved the radiochemical yield and radiotracer specific activity under all conditions of carrier NH_4Cl. As a comparison, we measured $[^{13}N]N_2$ specific activity derived from in-target production based on a 50 μA min irradiation driving the $^{14}N(p,pn)^{13}N$ reaction on a gaseous N_2 target. The 'wet' radiochemistry approach afforded two advantages over the in-target approach with a ~600-fold improvement in specific activity, and the ability to collect the tracer in a small volume of gas (~20 mL at STP).

Keywords: $[^{13}N]N_2$; nitrogen fixation; legumes

Introduction

Nitrogen is the key element that most often limits plant growth, productivity and crop quality in many agricultural ecosystems. Most plants assimilate nitrogen through uptake of nitrate or ammonium ions by their roots. However, legumes have the ability to fix atmospheric N_2 through an energetically expensive pathway involving a symbiosis in their roots with certain *Rhizobia* that manifest as nodules, or tiny appendages affixed to primary and lateral root structures belowground. Nitrogen fixation occurs through the action of bacterial nitrogenase and is strongly regulated as there is a potential for over-supply that would unbalance carbon and nitrogen metabolism within the plant.[1] Although early work suggests that nitrogen fixation is tightly coupled to carbon supply,[2,3] more recent studies have shown that its rate will often change in response to environmental cues (such as drought stress) before leaf-level photosynthetic capacity changes.[4–6] This raises the fundamentally important question of what regulates nitrogen fixation. In light of the growing concerns over climate change and how elevated atmospheric CO_2 and/or frequent drought conditions will impact our future agro-economy, there is a need to improve upon basic tools and technology that will enable the reliable measurement of these basic processes within intact plants.

Nitrogen-13 ($t_{1/2}$ 9.97 min), the only radioactive isotope of nitrogen, decays by positron emission. In today's age of medical imaging, this radioisotope can afford unique opportunities to conduct non-invasive imaging of intact plants enabling measurement of nodule activity associated with symbiotic nitrogen fixation, as well as redistribution of tracer into targeted tissues. More importantly, the short-lived nature of the isotope affords opportunity to retest same plants over time and prolonged exposure to environmental conditions giving opportunity to explore how plants rely on nitrogen input during growth and development while being stressed.

The subject of studying nitrogen input in N_2-fixing plants using short-lived radiotracers is not new, and in fact has been extensively reviewed.[7] Two prior works specifically address using $[^{13}N]N_2$ as a tracer.[8,9] These works showed not only that it was possible to measure uptake and redistribution of tracer within intact plants,[9] but that it was possible to observe changes in the radiolabeled metabolite profiles over time from tissue extracts.[8] Even so, plant scientists today tend to resort to using stable isotopes, and in particular $[^{15}N]N_2$ to study these dynamic processes, sacrificing the plant in order to measure the isotopic enrichment in selected tissues.[10] A less invasive approach relies on administering acetylene gas to the nodules, measuring the ethylene that evolves due to nitrogenase activity.[11] Even so, this approach can introduce confounding features to the integrated responses by the plant.

Historically, $[^{13}N]N_2$ as a tracer has been around for several decades, and used extensively in the context of studying pulmonary function both in animals and humans.[12] Several in-target methods have been described in the literature over the years, and are summarized in Table 1. Of course, neither radiotracer specific activity nor gas volume administered was of concern in these early pulmonary studies. Hence, there has not been much developmental research into improving these

[a]*Fachbereich Chemie, Johannes Gutenberg Universität, 55099 Mainz, Germany*

[b]*Brookhaven National Laboratory, Medical Department, Upton, NY 11973, USA*

**Correspondence to: Richard A. Ferrieri, Brookhaven National Laboratory, Medical Department, Upton, NY, USA 11973.*
E-mail: rferrieri@bnl.gov

Copyright © 2010 John Wiley & Sons, Ltd.

Table 1. In-target $[^{13}N]N_2$ production

Nuclear reaction	Target composition	Reference
$^{12}C(d,n)^{13}N$	CO_2 (*g*)	Clark and Buckingham[13]
$^{12}C(d,n)^{13}N$	Graphite (*s*)	
$^{16}O(p,\alpha)^{13}N$	CO_2 (*g*)	Murata *et al.*[14]
$^{13}C(p,n)^{13}N$	Amorphous ^{13}C	Ferrieri *et al.*[15]
$^{14}N(p,pn)^{13}N$	N_2 (*g*)	Le Bars[16]

qualities of the tracer. In legume studies, the small size of root nodules (typically less than 1 mm in diameter) and their limited number on a single plant places new constraints on the quality of the radiotracer to ensure adequate assimilation of radioactivity by the organism. Quite remarkably, there has been only one paper published that addresses these issues.[17] This work relied on a two-step process involving the reduction of $[^{13}N]NO_3^-$ using Devarda's Alloy in alkaline solution in step 1. The $[^{13}N]NO_3^{-1}$ was generated by bombarding a liquid water target with protons to induce the $^{16}O(p,\alpha)^{13}N$ nuclear reaction.

$$^{13}NO_3^- + \text{Devarda's Alloy (50\% Cu, 45\% A1, 5\% Zn)} \xrightarrow{KOH} {}^{13}NH_3 \quad (1)$$

In the step 2, $[^{13}N]NH_3$ was oxidized to $[^{13}N]N_2$ using a solution of hypobromite and carrier ammonium chloride.

$$^{13}NH_3 + {}^{14}NH_3 + 3NaOBr \rightarrow {}^{13}NN + 3NaBr + 3H_2O \quad (2)$$

Even so, the radiochemical yield and specific activity of the prepared $[^{13}N]N_2$ was not reported.

The aim of the present work was to explore how added carrier NH_4Cl and excess of hypobromite influenced the radiochemistry for making and rendering $[^{13}N]N_2$ in suitable states for plant studies. Further, we compared the characteristics of the radiotracer generated from this wet radiochemical approach with those from the in-target production of $[^{13}N]N_2$ via $^{14}N(p,pn)^{13}N$ reaction on a gaseous N_2 target.

Results and discussion

Throughout our studies, we fixed the amount of Devarda's alloy and KOH to ensure a near constant conversion of $[^{13}N]NO_3^-$ to $[^{13}N]NH_3$. Argon gas was also used to sparge ambient air from the system's plumbing and to facilitate distillation of $[^{13}N]NH_3$. We used three different amounts of NH_4Cl (0.2, 0.7l and 3.5 mmol) coupled with 1.6-fold and 6-fold molar equivalent excesses of hypobromite.

The radiochemical yield averaged 11.5% (based on starting $[^{13}N]NO_3^{-1}$ decay corrected to EOB), and the absolute specific activity averaged 2.5E−01 MBq μmol^{-1}. Typically, we were able to prepare ~259 MBq of gaseous $[^{13}N]N_2$ collected in the syringe in approximately 20 mL of gas (at STP) within 13 min from the end-of-bombardment (EOB) using 50 μA min of integrated beam on target (12.5 μA on target for 4 min irradiations).

Figure 1 shows the correlation between $[^{13}N]N_2$ radiochemical yield (decay corrected back to EOB) and its specific activity encompassing all aspects of the reaction conditions being tested. Data were greatly scattered owing to issues with quantitative transfer of $[^{13}N]NH_3$ between the Devarda's vessel and the oxidation vessel. Even so, we noted a weak positive correlation between radiochemical yield and tracer specific activity (Pearson's correlation coefficient, $r = 0.6204$). To understand this behaviour it was necessary to separate out the effects of each reaction parameter.

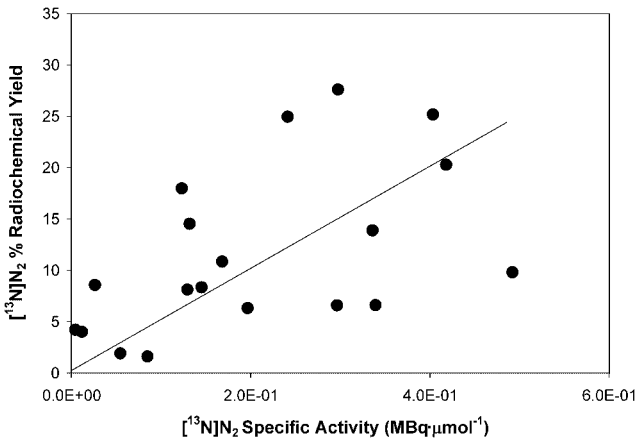

Figure 1. Plot of radiochemical yield (as % $[^{13}N]NO_3$ vs $[^{13}N]N_2$ specific activity (as MBq μmol^{-1}). A weak positive correlation is seen between these features (Pearson's correlation coefficient, r=0.6204).

Influence of the amount of carrier NH_4Cl and NaOBr on radiochemistry

The data in Figures 2(A–C) show how the two reaction parameters (carrier NH_4Cl and excess NaOBr) directly influenced radiotracer quality. As expected, increasing amounts of carrier NH_4Cl enhanced the radiochemical yield (Figure 2(A)), but not that drastically since a 17.5-fold increase in NH_4Cl only manifested in a ~2-fold increase in yield. However, we see a greater effect on radiochemical yield by increasing the amount of excess hypobromite than we do by increasing carrier NH_4Cl.

Furthermore, the increase in NH_4Cl reagent resulted in a ~10-fold increase in macroscopic N_2 (Figure 2(B)). However, increasing the amount of excess hypobromite from a 1.6-fold to a 6.0-fold molar excess did not increase the amount of N_2 produced. In fact, at 3.5 mmol NH_4Cl, an increase in the hypobromite molar excess resulted in a statistically significant drop in N_2 mass.

This behavior manifested in an interesting trend regarding $[^{13}N]N_2$ specific activity (Figure 2(C)). Comparison within subsets of data at 1.6 or 6.0 molar excess of hypobromite was not statistically different from each other at the 95% confidence level. However, there was a trend of increasing specific activity across subsets of data though not statistically relevant at the 95% confidence level. This trend at the higher molar excess of hypobromite was due to improvement of the radiochemical yield with a commensurate decrease in N_2 mass. As will be discussed in the following text, we believe the reason for this behavior might be attributed to poor mixing conditions in the oxidation vessel.

Our gas chromatographic analysis enabled measurement of gas composition and amounts of mass produced from the ensuing reactions. In addition to macroscopic amounts of N_2, we also saw O_2 in all samples collected. Molecular oxygen was thought to evolve from hypobromite decomposition.[18] Hypobromite is optimally stable at pH 11.4. However, the pH of the reaction solution will range from 4.5 to 5.5 depending on the amount of NH_4Cl introduced. Therefore, it is not surprising that

Copyright © 2010 John Wiley & Sons, Ltd.

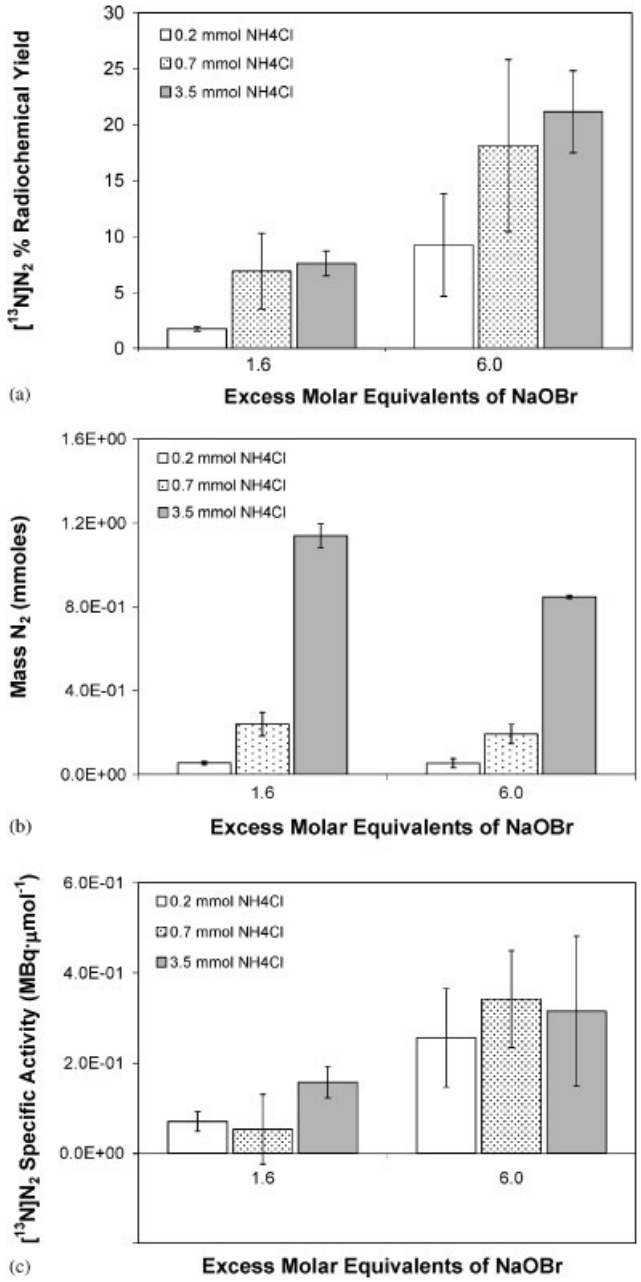

Figure 2. Panel A: Influence of carrier NH_4Cl and excess molar equivalents of NaOBr on $[^{13}N]N_2$ radiochemical yield. Panel B: Influence of carrier NH_4Cl and excess molar equivalents of NaOBr on total N_2 mass produced. Panel C: Influence of carrier NH_4Cl and excess molar equivalents of NaOBr on $[^{13}N]N_2$ specific activity. Error bars denote standard error on the mean value and reflect at least three replicates.

O_2 was generated in our process due to a lack of hypobromite stability. Even so, mass measurements indicated that the amounts of total O_2 produced were relatively constant (on average 2.5E−01 mmol) throughout all our studies (i.e. independent of the amounts of NH_4Cl or excess hypobromite introduced). Furthermore, we were unable to generate O_2 from simple decomposition of hypobromite using dilute HCl solutions that were adjusted to the same pH range as our radiochemistry. In light of this, we believe O_2 production must be intimately tied to the oxidation chemistry converting NH_3 to N_2, although we cannot offer detailed mechanistic insight at this time. Additionally, since O_2 production was independent of reagent

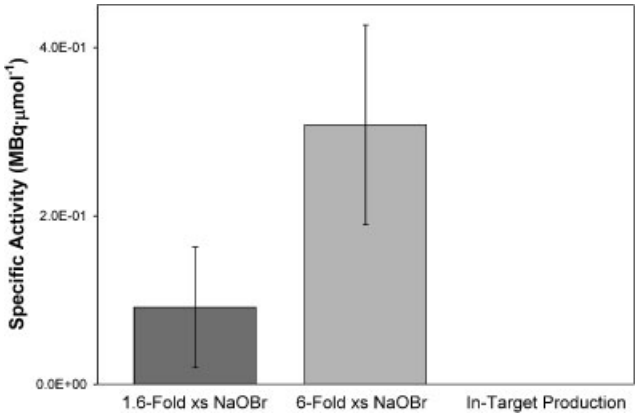

Figure 3. Comparison of $[^{13}N]N_2$ mean specific activities obtained using the wet chemistry approach (9.1E−02 MBq µmol^{-1} at 1.6-fold molar excess of hypobromite and 3.60E−01 MBq µmol^{-1} at 6-fold molar excess of hypobromite) and in-target approach (6.4E−04 MBq µmol^{-1}). Error bars reflect the standard deviation on the mean for at least three replicates.

strength, we believe that our hypobromite oxidation tube (see Experimental Section) might not have been homogeneously mixed during the addition of this reagent. As mentioned earlier, this lack of mixing could account for the positive correlation we observe (Figure 1) between radiochemical yield and radiotracer specific activity. Further studies are planned to test this hypothesis.

Wet chemistry vs in-target production

As we compared the wet chemistry data with the in-target production of $[^{13}N]N_2$ from routine ^{11}C production, we found that the wet chemistry approach offers clear advantages for plant research (Figure 3). We were able to attain on average a 600-fold improvement in the radiotracer's specific activity using the wet chemistry approach and formulate that tracer in approximately 20 mL of gas. Both features are important for its utility in plant science.

Comparative imaging of $[^{13}N]N_2$ and $[^{13}N]NH_3$ fixation in legumes

Legumes have the capacity to supplement their nitrogen input during growth by a microbial symbiosis that manifests in root nodules that are capable of fixing atmospheric nitrogen. Here we demonstrated the power of using the $[^{13}N]N_2$ tracer to image nitrogen fixation in soybean plants grown in rhizoboxes so that their roots were allowed to develop along the surface of the soil. A single administration of $[^{13}N]N_2$ to the root biomass showed substantial fixation of tracer within the root nodules (see Figure 4(A) for reference of nodule location on roots) and substantial allocation of $[^{13}N]$-labeled substrates throughout root system (Figure 4(B)). Intuitively, we expect a higher level of tracer input into targeted plant tissues using higher specific activity $[^{13}N]N_2$. However, nitrogen fixation can be relatively efficient in legumes as Meeks *et al.*[8] and Caldwell *et al.*[9] demonstrated. In those early studies, relatively low specific activity $[^{13}N]N_2$ derived from in-target production sources was used, yet efficient uptake and redistribution of tracer to other tissues was noted. For assessing changes in resource allocation at organism scales, likely low specific activity $[^{13}N]N_2$ is adequate. However, for more specialized studies designed to measure ^{13}N-partitioning into distinct metabolic pools both

Copyright © 2010 John Wiley & Sons, Ltd.

Figure 4. Panel A shows a picture of the soybean plant after careful removal from its growth box. The white arrows in the picture show where nodule development had occurred. Panel B shows a phosphor plate image of the root biomass after $[^{13}N]N_2$ administration. Lighter areas depict high levels of radioactivity. Note the correspondence of nodule biomass with high radioactivity. Panel C shows a phosphor plate image of the same rhizobox after $[^{13}N]NH_3$ administration. Note that tracer becomes fixed in the soil at the site of introduction.

within the nodules and in other sink tissues, the higher specific activity tracer will provide an added advantage by enabling higher incorporation of radioactive isotope per mass of tissue.

As a further assurance that $[^{13}N]NH_3$, as a potential contaminant in the $[^{13}N]N_2$ formulation, was not contributing to the image seen in Figure 4(B), we introduced a pulse of $[^{13}N]NH_3$ gas to the same rhizobox (Figure 4(C)). This tracer appeared fixed in the soil at the site of introduction. Therefore, we are assured that tracer fixation and transport seen in Figure 4(B) is a reflection of $[^{13}N]N_2$ involvement.

Summary

In summary we were able to optimize the process to achieve reasonable amounts of pure $[^{13}N]N_2$ radiotracer suitable for plant assimilation studies using higher amounts of both carrier NH_4Cl and hypobromite. The O_2 evolved from the process will not interfere with the nitrogen fixation capacity of the plant root nodules. We believe the higher quality of tracer produced by this method (i.e. higher specific activity) will afford unique opportunities to explore plant utilization of nitrogen in key metabolic pathways for growth and development.

Experimental

Materials and methods

Wet chemistry approach: Nitrogen-13 was produced via the $^{16}O(p,n)^{13}N$ nuclear transformation using distilled water in a 2.5 mL volume high-pressure liquid target and 18 MeV protons on the front foil (15.5 MeV on target for 50 μA min: 12.5 μA on target for 4 min) on the TR-19 (Ebco Industries Ltd., Richmond, BC, Canada) cyclotron at Brookhaven National Laboratory. The nitrogen-13 was recovered in the hot lab (Figure 5) as $[^{13}N]NO_3^-$ and chemically reduced to $[^{13}N]NH_3$ gas using about 4 g Devarda's Alloy (Aldrich Chemical, St. Louis, MI, USA) with 350 mg of crushed KOH pellets (Mallinckrodt, Phillipsburg, NJ, USA).[19] Because of the long transfer line from target to hot lab, it was necessary to first collect the water, and then introduce it as a bolus to the Devarda's vessel A. Within 3 min of EOB, we were able to recover an average of 2035 MBq of $[^{13}N]NO_3^-$.

The progress of both irradiated water collection and Devarda's reaction was monitored using a PIN diode radiation detector (Bioscan Inc., Washington, DC, USA) that was strategically located between the collection vessel and vessel B. Once the $[^{13}N]NO_3^-$ arrived at vessel B, heat was applied using a hot air gun until the reaction showed signs of initiation. The $[^{13}N]NH_3$ was distilled under argon flow through a Teflon 3-way valve, and trapped in vessel C containing 0.7 mL volume of DI water containing various amounts of NH_4Cl (>99.5%, Aldrich Chemical). The tubing between those vessels was washed with bicarbonate solution and dried under argon to prevent sticking of $[^{13}N]NH_3$ during transfer. A second PIN diode radiation detector monitored the progress of the process. At the completion of $[^{13}N]NH_3$ trapping, vessel B was vented to a Sicapent™ trap (P_2O_5, Aldrich Chemical) and NaOBr solution was remotely introduced into vessel C, which was prepared according to the procedure by Vaalburg *et al.*[17] During oxidation, the evolving $[^{13}N]N_2$ gas filled a disposable 60 mL syringe equipped with a shut-off valve (BD, Franklin Lakes, NJ, USA). Unreacted $[^{13}N]NH_3$ was trapped with an additional Sicapent™ column preventing it from contaminating the collected tracer in the syringe. The material in this column was replaced with every run. Once filled, the syringe was counted for total radioactivity using a Capintec Dose Monitor (Capintec Inc., Ramsey, NJ, USA), and a 0.1 mL volume aliquot was withdrawn for radio gas chromatography analysis.

Analyses of collected gas were carried out using a 5860A gas chromatograph (Hewlett Packard, Houston, TX, USA) equipped with a Spherocarb column (1/8-in o.d. × 10-ft stainless steel, 80/100 mesh: Alltech, Deerfield, IL, USA) coupled to a thermal conductivity detector (TCD). The system was operated isothermally using helium carrier gas at 30 mL min^{-1} and maintaining instrument zones to the following: injector (42°C); column oven (24°C); and TCD (250°C). The outflow of the TCD was connected in series with a Geiger counter (Ludlum Technologies,

Copyright © 2010 John Wiley & Sons, Ltd.

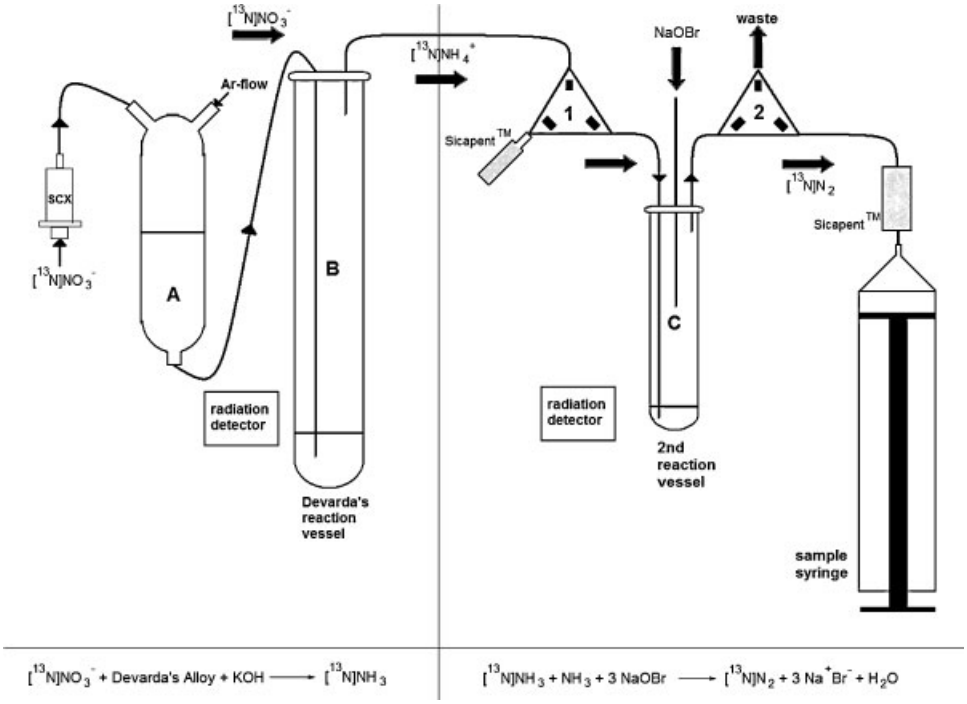

Figure 5. Schematic showing the plumbing arrangement for collecting $[^{13}N]NO_3^-$ from the target, reducing it to $[^{13}N]NH_3$ and oxidizing it to $[^{13}N]N_2$. Note that a strong cation exchange cartridge (Waters, Milford, CT, USA) was used on the initial collection of $[^{13}N]NO_3^-$ to ensure removal of vanadium-48 by-product from the target.

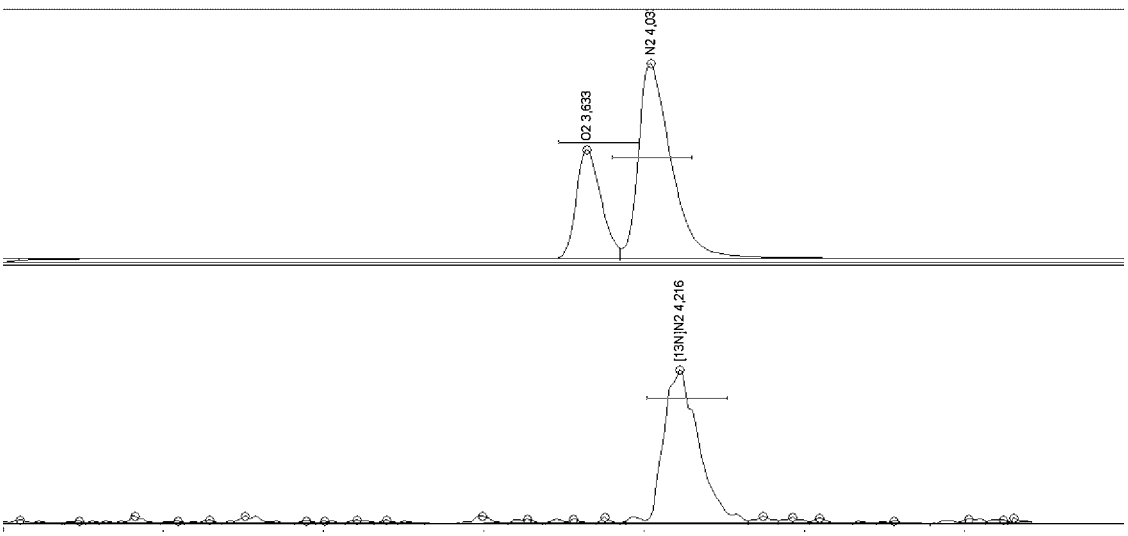

Figure 6. Example of a radio-gas chromatograph showing mass elution profiles (O_2 at 3.72 min and N_2 at 4.14 min) and radioactive $[^{13}N]N_2$ at 4.22 min). The slight lag in the radioactivity peak was due to the Geiger Counter being plumbed in series after the thermal conductivity mass detector. Note the higher levels of O_2 present than in ambient air owing to an *in situ* source of O_2 from hypobromite.

Sweetwater, TX, USA) enabling direct measurements of mass and associated radioactivity. Analog outputs from the mass and radioactivity detectors were acquired using a SRI chromatography acquisition station (SRI Instruments, Torrance, CA, USA). Peaks were integrated using PeakSimple™ software (SRI Instruments) on that system. A mass calibration of the TCD response was carried out using N_2 and O_2 standards so that integrated peaks could be converted to mmoles of mass. A ten-point mass calibration curve of each component yielded linear correlations ($R^2 > 0.99$). The Geiger counter was also cross-calibrated against a 4πNaI gamma counter (3 in o.d. crystal, Quantum, MCA2100R, Princeton Gamma-Tech Instruments, East Princeton, NJ, USA) using a NIST traceable Ge-68 source. All ^{13}N data were decay corrected to EOB.

In one instance, gas analysis was carried out using a Porapak N column (1/8-in o.d. × 6-ft stainless steel, 80/100 mesh: Alltech) to verify that $[^{13}N]NH_3$ was removed by the Sicapent™ stripping column during $[^{13}N]N_2$ collection. The column was operated isothermally at 50°C using a helium carrier gas flow of 50 mL min^{-1}.

Copyright © 2010 John Wiley & Sons, Ltd.

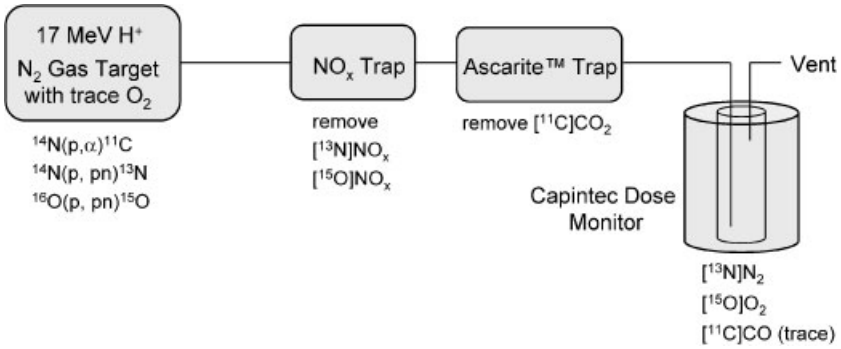

Figure 7. Schematic showing the plumbing layout with in-line traps for scavenging unwanted radioactive target components. The $[^{13}N]N_2$ collection bulb was a 2 L bulb that fit inside a Capintec Dose Monitoring chamber. Sampling was halted once radioactivity within this collection bulb reached a maximum value.

Figure 6 shows a typical mass and radioactivity trace of a sample taken from the wet chemistry collection syringe. The only radioactive component in the gas mixture was $[^{13}N]N_2$. Macroscopic amounts of N_2 and O_2 were detected, as well.

In-target production approach: $[^{13}N]N_2$ was produced *via* the $^{14}N(p,pn)^{13}N$ reaction occurring during the $^{14}N(p,\alpha)^{11}C$ carbon dioxide production with a N_2 gas target (50 mL volume at 400 psi N_2) and 18 MeV protons on the front target foil (15.5 MeV on gas). Figure 7 shows the system layout for trapping unwanted target components and sampling $[^{13}N]N_2$. Aliquots for radio GC analysis were withdrawn directly from the collection bulb after measuring the total activity. Typically, a 50 μA min irradiation (25 μA on target for 2 min) would produce 148 MBq of $[^{13}N]N_2$ in 2 L of N_2 gas at STP. Radio gas chromatography analysis using the Spherocarb column revealed a small amount of $[^{15}O]O_2$ as a contaminant.

Tracer administration: Soybean seeds (Edamame, *Glycine max*.(L.) Merr.; Johnny's Seed Co., Winslow, Maine USA) were inoculated with bacterium and allowed to germinate on wetted foam pads. Once germinated, plants were transferred to $6 \times 6 \times 0.5$ in plastic boxes filled with screened soil, covered with a plastic lid and inverted at a 45° angle to force the roots to grow along the top surface of the soil. Plants were grown under a 16/8 photoperiod using Agro lights (300 $\mu mol\, m^{-2}\, s^{-1}$) and watered on a 3-day cycle. Nutrient, depleted of extraneous nitrogen, was administered weekly. The lack of nitrogen forced nodules to quickly grow on the roots.[20]

$[^{13}N]N_2$ was administered to the rhizobox through a valve located at the center of the box's cover. Once administered, the tracer was allowed to incubate for 2 min prior to sparging the box with ambient air (100 $mL\, min^{-1}$) for an additional 4 min. At this point, the cover to rhizobox was removed and the entire root mass subjected to positron autoradiography (Fuji BAS 2500 Imager) exposing a phosphor plate for 3 min. The plate was laid across the soil surface of the opened rhizobox, enabling direct contact with the root system. A glass plate was pressed on top of the phosphor plate during exposure to ensure uniform contact.

$[^{13}N]NH_3$ gas was administered slightly differently than described above. For this test, the tracer was distilled from the DaVarda's reactor using an air flow of 400 $mL\, min^{-1}$ that enabled transfer across a 50 ft length of 1/8″o.d. Teflon tubing connected directly to the rhizobox via the cover valve.

Acknowledgements

This research was supported in part by the US Department of Energy, Office of Biological and Enviromental Research under contract DE-AC02-98CH10886, and in part by Deutscher Akademischer Austauschdienst (DAAD), Bonn for a student fellowship (supporting Kasel).

References

[1] R. Parsons, R. J. Sunley, *J. Exp. Bot.* **2001**, *52*, 435–443.
[2] R. J. Lawn, W. A. Brun, *Crop Sci.* **1974**, *14*, 11–16.
[3] G. L. Benthenfalvay, S. S. AbuShakra, K. Fishbeck, D. Phillips, *Physiologia Plantarum.* **1978**, *43*, 31–34.
[4] T. Kuo, L. Boersma, *Agronomy J.* **1971**, *63*, 901–904.
[5] T. R. Sinclair, *Field Crop Res.* **1986**, *15*, 125–141.
[6] J. L. Durand, J. E. Sheehy, P. R. Minchin, *J. Exp. Bot.* **1987**, *38*, 311–321.
[7] K. R. Schubert, G. T. III Coker, Nitrogen and carbon assimilation in N_2-fixing plants: short-term studies using ^{13}N and ^{11}C. in Advances in Chemistry, Vol. 197, chapter 16, ACS Publications, Washington, DC, **1981**, pp. 317–339.
[8] J. C. Meeks, C. P. Wolk, N. Schilling, P. W. Shaffer, *Plant Physiol.* **1978**, *61*, 980–983.
[9] C. D. Caldwell, D. S. Fensom, L. Bordeleau, R. G. Thompson, R. Drouin, R. Didsbury, *J. Exp. Bot.* **1984**, *35*, 431–443.
[10] T. E. Dawson, S. Mambelli, A. H. Plamboeck, P. H. Templer, K. P. Tu, *Annu. Rev. Ecol. Syst.* **2002**, *33*, 507–559.
[11] W. Stewart, G. Fitzgerald, R. Burris, *Proc. Natl. Acad. Sci. USA* **1967**, *58*, 2071–2078.
[12] J. Nosil, J. M. B. Hughes, F. R. Hudson, M. J. Myers, P. W. Ewan, *Phys. Med. Biol.* **1976**, *21*, 251–262.
[13] J. C. Clark, P. D. Buckingham, Short-lived radioactive gases for clinical use, chapter 6, Butterworth & Co. (Publisher) Ltd., **1975**, pp. 171–191.
[14] K. Murata, H. Itoh, M. Senda, G. Todo, Y. Yonekura, K. Torizuka, *Radiology* **1986**, *158*, 303–307.
[15] R. A. Ferrieri, D. J. Schlyer, B. W. Wieland, A. P. Wolf, *Int. J. Appl. Radiat. Isot.* **1983**, *34*, 897–900.
[16] D. Le Bars, *J. Label. Compd. Radiopharm.* **2001**, *44*, 1–5.
[17] W. Vaalburg, A. Steenhoek, A. M. J. Paans, R. Peset, S. Reiffers, M. G. Woldring, *J. Label. Compd. Radiopharm.* **1981**, *18*, 303–308.
[18] D. B. Sprinson, D. Rittenberg, *J. Biol. Chem.* **1949**, *180*, 707–714.
[19] R. A. Ferrieri, A. P. Wolf, *Radiochim. Acta.* **1983**, *34*, 69–83.
[20] R. W. F. Hardy, U. D. Havelka, Photosynthate as a major factor limiting N-fixation by field-grown legumes with emphasis on Soybeans. in *Nitrogen Fixation in Plants* (Ed.: P. S. Nutman), Cambridge University Press, Cambridge, **1977**, pp. 421–439.

Copyright © 2010 John Wiley & Sons, Ltd.